Broadband photocarrier dynamics and nonlinear absorption of PLD-grown WTe_2 semimetal films

Wenbin Gao, Lei Huang, Jinlong Xu, Yequan Chen, Chunhui Zhu, Zhonghui Nie, Yao Li, Xuefeng Wang, Zhenda Xie, Shining Zhu, Jun Xu, Xiangang Wan, Chao Zhang, Yongbing Xu, Yi Shi, and Fengqiu Wang

Citation: Appl. Phys. Lett. **112**, 171112 (2018); doi: 10.1063/1.5024777

View online: https://doi.org/10.1063/1.5024777

View Table of Contents: http://aip.scitation.org/toc/apl/112/17

Published by the American Institute of Physics

Broadband photocarrier dynamics and nonlinear absorption of PLD-grown WTe_2 semimetal films

Wenbin Gao,[1,2] Lei Huang,[1,2] Jinlong Xu,[1,2] Yequan Chen,[1,2] Chunhui Zhu,[1,2] Zhonghui Nie,[1,2] Yao Li,[1,2] Xuefeng Wang,[1,2] Zhenda Xie,[1,2] Shining Zhu,[2,3] Jun Xu,[1,2] Xiangang Wan,[2,3] Chao Zhang,[4] Yongbing Xu,[1,2] Yi Shi,[1,2] and Fengqiu Wang[1,2,a)]
[1]*School of Electronic Science and Engineering, Nanjing University, Nanjing 210093, China*
[2]*Collaborative Innovation Center of Advanced Microstructures, Nanjing University, Nanjing 210093, China*
[3]*School of Physics, Nanjing University, Nanjing 210093, China*
[4]*School of Physics and Institute for Superconducting and Electronic Materials, University of Wollongong, New South Wales 2522, Australia*

(Received 4 February 2018; accepted 15 April 2018; published online 27 April 2018)

WTe_2 is a unique material in the family of transition metal dichalcogenides and it has been proposed as a candidate for type-II Weyl semimetals. However, thus far, studies on the optical properties of this emerging material have been significantly hindered by the lack of large-area, high-quality WTe_2 materials. Here, we grow a centimeter-scale, highly crystalline WTe_2 ultrathin film (~35 nm) by a pulsed laser deposition technique. Broadband pump-probe spectroscopy (1.2–2.5 μm) reveals a peculiar ultrafast optical response where an initial photo-bleaching signal (lasting ~3 ps) is followed by a long-lived photoinduced absorption signature. Nonlinear absorption characterization using femtosecond pulses confirms the saturable absorption response of the WTe_2 ultrathin films, and we further demonstrated a mode-locked Thulium fiber laser using a WTe_2 absorber. Our work provides important insights into linear and nonlinear optical responses of WTe_2 thin films. *Published by AIP Publishing.*
https://doi.org/10.1063/1.5024777

Recently, semimetals whose low-energy electrons are characterized by a massless linear dispersion have drawn considerable attention across the fields of condensed matter physics and optoelectronics.[1–3] Apart from being a platform for exploring exotic fundamental physics, the unique band structures and photo-excitations make these materials particularly relevant to photonic applications in the mid-infrared bands. Investigation of the optical properties of these emerging semimetals has concentrated on using ultrafast optical pump-probe techniques to reveal their hot carrier dynamics. For example, it has been demonstrated that cadmium arsenide (Cd_3As_2), a three-dimensional Dirac semimetal, exhibits a broadly tunable photocarrier lifetime in the mid-wave infrared (3–6 μm), as driven by symmetry-breaking induced gap-opening.[4–6] Optoelectronic devices such as fast photodetectors with promising figures-of-merit were also realized using cadmium arsenide.[7,8]

Transition metal dichalcogenide WTe_2, also deemed a type-II Weyl semimetal candidate, exhibits extraordinary properties such as large unsaturated magnetoresistance (MR) and exotic superconducting behaviour under high pressure.[9,10] Pump-probe spectroscopy of bulk single-crystal WTe_2 has revealed two ultrafast relaxation components.[11] In addition, thickness-dependent photocarrier dynamics was experimentally identified and was linked to the evolution of the band structures.[12] The very fast relaxation of photocarriers in WTe_2 makes it suitable for ultrafast pulse generation. Indeed, femtosecond pulse generation in fiber lasers mode-locked by a saturable absorber (SA) based on bulk-structured WTe_2 microflakes has been reported.[13] A clear drawback is that the flakes are quite defective and do not form a continuous film in the lateral direction. For a range of optoelectronic applications, it is highly desirable to synthesize functional materials in the form of ultrathin films, which would greatly facilitate device design and fabrication. Despite the immense importance, fabrication of large-area, high-quality WTe_2 ultrathin films is only recently demonstrated, and knowledge about the basic optical properties of such films remains elusive.[14] In the meantime, there is increasing motivation to understand the photocarrier dynamics at relatively long wavelengths and to develop Dirac fermion enabled optoelectronic devices.[4] However, most of the existing pump-probe studies have employed probe photons well exceeding the Dirac cone energy range.[11,12,15]

In this work, we grow a centimeter-scale, uniform, and highly crystalline WTe_2 ultrathin film (~35 nm) by a pulsed laser deposition technique. Non-degenerate pump-probe spectroscopy is carried out with a broadly tunable probe wavelength, varying from 1.8 to 2.5 μm. Both wavelength and fluence dependent measurements reveal a highly unified transient response, where a picosecond ultrafast photo-bleaching (PB) signature is followed by a much slower photoinduced absorption (PA) component. Such a response is appreciably different from the results obtained for bulk WTe_2 materials. In addition, strong saturable absorption is verified using nonlinear absorption characterization and we experimentally demonstrated a Thulium fiber laser mode-locked with the WTe_2 absorber at 2 μm. Our results indicate that WTe_2 ultrathin films are promising for long-wavelength optical switches, with complementary characteristics found in other Dirac materials, such as Cd_3As_2.

Pulsed laser deposition (PLD) is an outstanding technique for preparing large-scale thin films. Here, we grew a WTe_2 thin film with an ~35 nm thickness on a mica

a)Email: fwang@nju.edu.cn

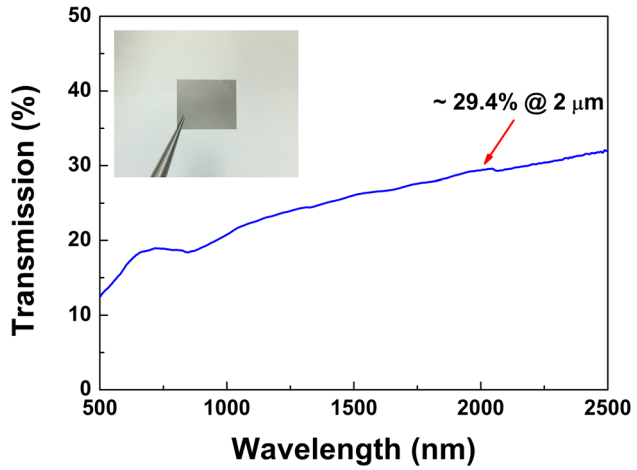

FIG. 1. Linear optical characterization of the WTe_2 thin film. Linear transmission of the WTe_2 thin film on mica substrate. The inset shows a photograph of the WTe_2 sample.

substrate followed by the annealing process.[14] The sample, which contains about 24 monolayers of WTe_2, is first characterized by X-ray photoemission spectroscopy (XPS) to confirm the stoichiometry (Fig. S1). X-ray diffraction (XRD) is performed to characterize the crystal quality of the prepared sample. As shown in Fig. S2(a), the diffraction peaks for the {001} crystal planes of WTe_2 can be well resolved and no other plane peaks are found (the un-indexed peaks come from the mica substrate), indicating that the sample had a nearly perfect c-axis orientation (see supplementary material). Figure S2(b) shows the Raman spectrum of the WTe_2 sample. The five observed peaks agree well with the previous reports, further confirming the good crystallinity of the thin film sample.[14,16] Transmission electron microscopy (TEM) characterization also proves the single-crystalline structure of the WTe_2 thin film, as shown in Fig. S3.

We first study the linear optical properties of the as-grown WTe_2 film by measuring the transmission spectra using a UV-Vis-IR spectrophotometer (UV-3600), as shown in Fig. 1. The transmittance of the film becomes larger as the wavelength increases, which is consistent with previous experimental results.[15] This is also qualitatively consistent with calculated transmission spectra based on density-functional theory (DFT) (Fig. S4), and the signatures at ~650 nm and ~1100 nm are both due to transitions between the W-5d and Te-5p bands. The relatively small transmittance is attributed to the surface reflection as well as the influence of the relatively thick mica substrate. The photograph (Fig. 1 inset) and the AFM results (Fig. S5) illustrate both the good surface morphology and flatness in the prepared film. To investigate the ultrafast photocarrier dynamics of WTe_2 thin films, non-degenerate pump-probe spectroscopy was performed using a 1 kHz 100 fs Ti: Sapphire amplifier system.[4] A typical pump-probe trace with an 800 nm pump and a 2 μm probe is shown in Fig. 2(a). It is found that the signal exhibits an initial photo-bleaching (PB), followed by a photoinduced absorption (PA) signature lasting over several hundreds of picoseconds. Such general observation holds for a pump fluence range of 100–300 $\mu J/cm^2$ (Fig. S6). Moreover, a pure mica substrate does not have any transient response under the same conditions. The fast PB decay, occurring within a picosecond timescale (~2.9 ps), is typically associated with the carrier-phonon cooling process.[11] To confirm the origin of the PA, we further performed wavelength dependent measurements. The linear increase in the peak signal with the pump fluence [inset of Fig. 2(a)] indicates that the pump-probe experiment is within the linear, unsaturated regime, ruling out effects from two-photon absorption. Figure 2(b) shows the broadband transient absorption measurement when the probe is tuned from 1.8 to 2.5 μm. Very similar dynamics were observed over the entire range. The presence of broadband and unifying feature means that linewidth broadening effects, which typically involve the change of signal polarity at a specific transition photon energy, do not play a major role.[17–19] We further confirmed the experimental observation by carrying out pump-probe spectroscopy using an 80 MHz Ti:Sapphire OPO system, and the results with a probe wavelength down to 1.2 μm show qualitatively very similar response (Fig. S7). Based on these results, we attribute the PA signal to the effect from surface related defects and trap states. Indeed, similar PB to PA transition due to carrier trapping has

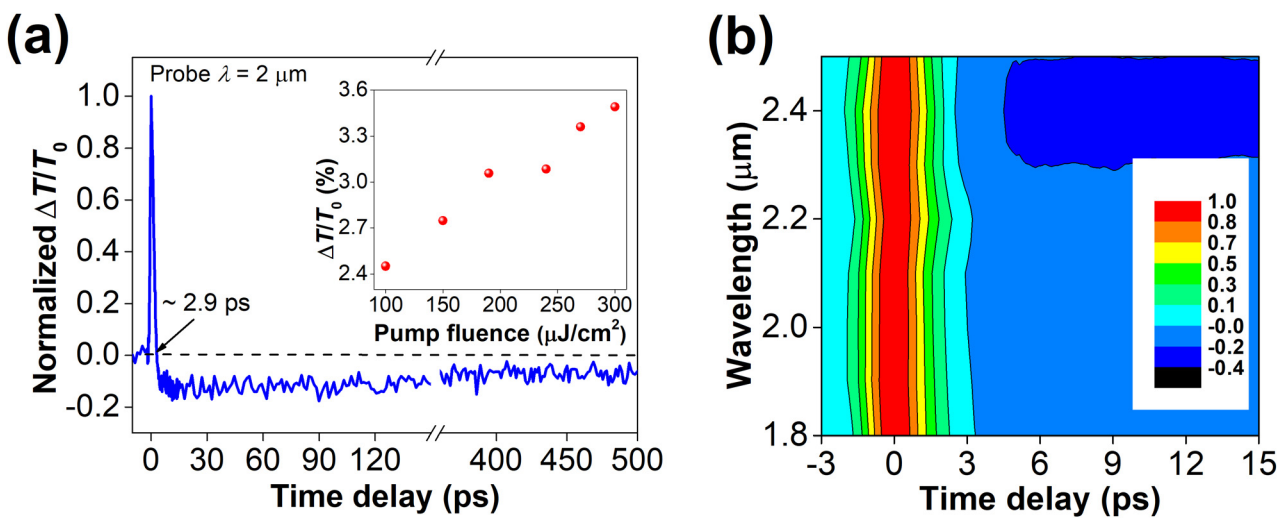

FIG. 2. (a) Transient transmission of the WTe_2 thin film sample with an 800 nm pump and a 2000 nm probe. Inset: increasing peak value of $\Delta T/T_0$ as a function of pump fluence (b) Normalized $\Delta T/T_0$ with the probe varying from 1.8 to 2.5 μm at a pump fluence of 300 $\mu J/cm^2$.

been observed before in monolayer MoS_2 samples, as well as conventional semiconductors.[20,21] It should be noted that such a long-lived "offset" signature can also be caused by heat diffusion effects.[11,22,23] Further studies, desirably on samples with varying defect concentrations, are necessary to fully elaborate the origin of the observed PA effect. In any case, the dynamics results present herein unambiguously support that the PLD-grown WTe_2 thin film can act as a fast saturable absorber for building ultrafast mode-locked lasers across the entire 1.2–2.5 μm range.

For the short-pulse generation experiment, the WTe_2 thin film was mechanically exfoliated from the thick mica substrate and sandwiched between two Ferrule Connector/Physical Connection (FC/PC) fiber connectors to form a fiber adapter saturable absorber. The nonlinear absorption measurement of the WTe_2 SA was performed by a power-dependent transmission technique, employing a carbon nanotube mode-locked fiber laser. The mode-locked laser was operating at 1.96 μm with a pulsewidth of ~700 fs and a repetition rate of 24 MHz. A digital variable optical attenuator (VOA) (OZ OPTICS) was used to change the optical power. The output of the laser was split into two arms by a 40/60 coupler. The 40% port was used as reference, while the 60% port was used to pump the WTe_2 SA. Afterwards, the material's transmission was tested under different optical powers. The typical nonlinear absorption curve of the tested sample at 1.96 μm is shown in Fig. 3. The relationship between the optical transmission and the input laser power was fitted by a simple saturable absorption model with the form

$$T(I) = 1 - \Delta T \exp\left(\frac{-I}{I_{sat}}\right) - T_{ns},$$

where $T(I)$ is the transmission, ΔT is the modulation depth, I is the incident peak intensity, I_{sat} is the saturation peak intensity, and T_{ns} is the non-saturable loss. The saturable peak intensity, modulation depth, and non-saturable loss are retrieved to be 1.1 MW/cm^2, 8.4%, and 35.7%, respectively. Although there are PA signatures in the photocarrier relaxation dynamics, the fact that the nonlinear absorption using femtosecond pulses only probes the very early-stage of the sample dynamical response renders the results shown in Fig. 3 highly reasonable.[24] It was worth noting that the saturable intensity of WTe_2 is relatively small compared to other saturable materials such as MoS_2 and Bi_2Te_3.[25,26] The damage threshold of the WTe_2 thin film is measured to be ~143 GW/cm^2 at a wavelength of 2 μm.

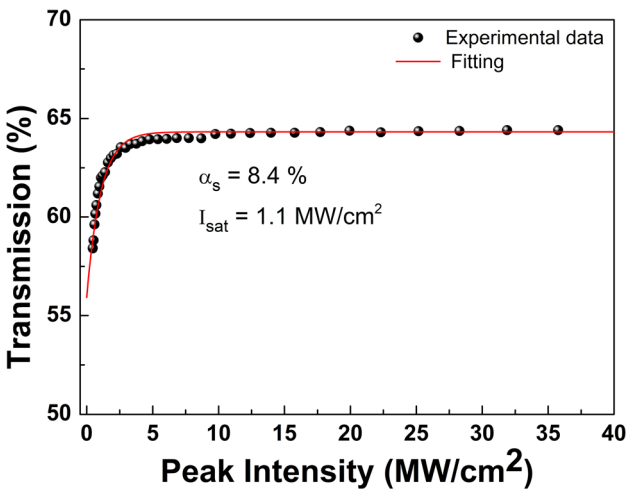

FIG. 3. Nonlinear absorption measurement. Measured nonlinear saturable absorption curve of the WTe_2 SA at 1.96 μm. A modulation depth of ~8.4% and a saturation intensity of 1.1 MW/cm^2 are deduced.

In order to confirm the feasibility of using the as-prepared WTe_2 SA for laser mode-locking, we constructed a Tm/Ho fiber laser as illustrated in Fig. 4. The pump source was from a 1550 nm laser diode amplified by a commercial erbium-doped fiber amplifier (EDFA) (PriTel, FA-30-IO), which has a maximum output power of 1 W. The pump source was coupled to the laser cavity though a 1550/2000 nm wavelength-division-multiplexer (WDM). A 2.1-meter-long Tm/Ho co-doped single-mode fiber (CorActive, TH512) with an ~12 dB/m (at 1550 nm) absorption coefficient was used as the gain medium. A polarization-insensitive isolator (PI-ISO) was placed in the cavity to ensure unidirectional operation. 10% of the light was extracted from the cavity as the output via a 10/90 coupler (OC). For finely optimizing the mode-locking state, an in-line polarization controller (PC) was employed to adjust the intra-cavity polarization state. Then, the WTe_2 film sample sandwiched between two fiber connector ends was inserted as the mode-locker.

In the experiment, when we slowly increased the pump power and carefully adjusted the polarization controller, stable self-started mode-locked pulses were observed at a pump power threshold of 158 mW. Under the pump power, the average output power was 1.17 mW. Compared with other two-dimensional materials such as MoS_2 and black phosphorus for fiber laser mode-locking in the soliton regime in previous reports, the threshold power is much lower, mostly due to its low saturable intensity. To testify that the mode-locking was started and sustained by the WTe_2 SA, we removed the WTe_2 film on the fiber ferrule. No mode-locking pulse was observed no matter how we changed the pump power and adjusted the polarization controller. Therefore, it proves that the WTe_2 thin film is indeed the mode-locking device in the Tm/Ho fiber laser.

To characterize the mode-locked Tm/Ho fiber laser, the output pulse train was first detected by a 12.5-GHz InGaAs Photodiode (EOT, ET-5000F) and a 500 MHz digital oscilloscope (Agilent, DSO-X 3052A). Figure 5(a) shows the recorded oscilloscope trace over a 180 ns time span. The interval of

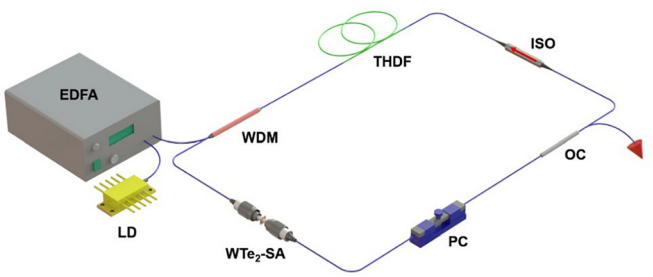

FIG. 4. Experimental setup of the mode-locked Tm/Ho fiber laser with WTe_2-SA. LD: laser diode, EDFA: erbium-doped fiber amplifier, WDM: wavelength-division multiplexer, THDF: Thulium-Holmium co-doped fiber, ISO: isolator, WTe_2-SA: WTe_2 saturable absorber, PC: polarization controller, and OC: output coupler.

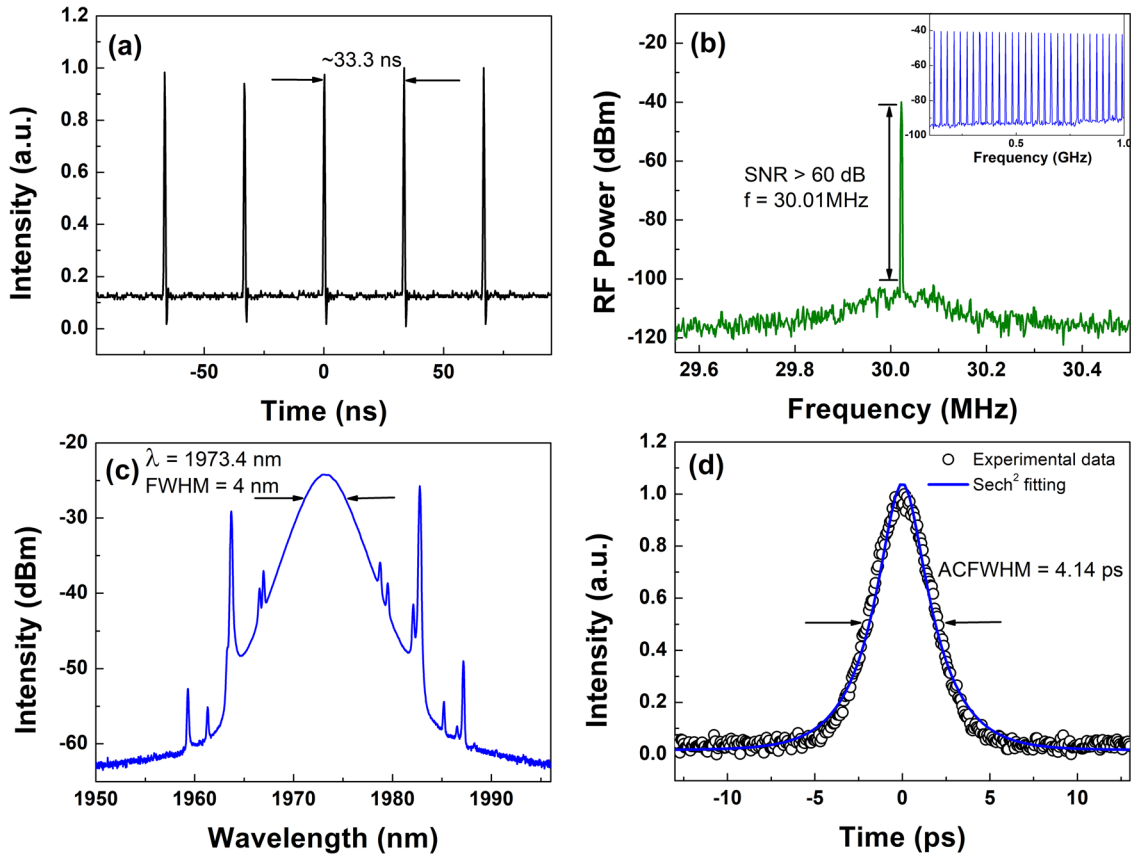

FIG. 5. Mode-locked laser characteristics. (a) Mode-locked pulse train from the oscilloscope. (b) RF spectrum with a 1 MHz span and a 1 kHz resolution bandwidth. Inset: RF spectrum over a span of 1 GHz. (c) Typical optical spectrum with a FWHM bandwidth of ~4 nm. (d) Autocorrelation trace and fitting $Sech^2$ shape pulse.

adjacent pulses is ~33.3 ns, which corresponds to a pulse repetition rate of 30.01 MHz. The recorded repetition rate matches well with the total cavity length of about 6.7 m. Meanwhile, to study the stability of the mode-locking state, the RF spectrum of the detected signal was analyzed using a 3-GHz radio frequency spectrum analyzer (R&S, FSC3). The RF spectrum is shown in Fig. 5(b) with a resolution bandwidth (RBW) of 1 kHz and a scanning range of 1 MHz. The signal-to-noise ratio (SNR) of the fundamental frequency signal is 62 dB; meanwhile, in the inset of Fig. 5(b), within a frequency span of 1 GHz, no amplitude modulation is observed, indicating good stability of the continuous-wave mode-locking.

The spectrum of the mode-locked pulses was characterized using an optical spectrum analyzer (Yokogawa, AQ6375) with a spectral resolution of 0.05 nm. Figure 5(c) shows a typical optical spectrum of the mode-locked Tm/Ho fiber laser. The spectrum has a center wavelength of 1973.4 nm and a full width at half maximum (FWHM) bandwidth of 4 nm. The Kelly sidebands can be clearly observed on the spectrum which is typical for the laser operating in the soliton regime.

At last, we used a mid-infrared autocorrelator (APE, Pulsecheck MIR) to measure the pulse width of the mode-locked pulses. Due to the relatively low sensitivity of the second harmonic generation (SHG)-based autocorrelator, a thulium-doped fiber amplifier was used to boost the power of the oscillator to 100 mW. The autocorrelation trace of the amplified mode-locked laser is depicted in Fig. 5(d), which has a FWHM of 4.14 ps. Assuming a $sech^2$ pulse profile, the corresponding pulsewidth is 2.7 ps. The time-bandwidth product (TBP) is calculated be to be 0.83, larger than the Fourier transform limit because of the unavoidable broadening during the amplification process.

In summary, the optical properties of a large-area, PLD-grown WTe_2 ultrathin film are investigated. It is found that the semimetal thin film exhibits a pronouncedly different ultrafast response compared with the bulk materials, where a fast PB signal due to saturable absorption is followed by a prolonged PA signal. Such a response persists over a broad spectral range, at least covering 1.2 to 2.5 μm, and makes WTe_2 an efficient fast saturable absorber. The saturation intensity is desirably lower than other Dirac semimetals, i.e., Cd_3As_2. We have experimentally demonstrated a passively mode-locked Tm/Ho fiber laser mode-locked by WTe_2 SA. The center wavelength, spectral bandwidth, pulse width, and repetition rate were 1973.4 nm, 4 nm, 2.7 ps, and 30 MHz, respectively. Our work reveals the potential of Weyl semimetals in ultrafast photonic applications.

See supplementary material for more characterizations of the sample.

This work was supported in part by the National Key R&D Program of China (2017YFA0206304); the National Basic Research Program of China (2014CB921101 and 2011CB301900); National Natural Science Foundation of China (61775093, 61378025, and 61427812); National Young 1000 Talent Plan; A "Jiangsu Shuangchuang Team"

Program; Jiangsu NSF (BK20170012 and BK20140054); and Australian Research Council (DP 160101474).

[1]J. M. Shao and G. W. Yang, AIP Adv. **5**, 117213 (2015).
[2]C.-K. Chan, N. H. Lindner, G. Refael, and P. A. Lee, Phys. Rev. B **95**, 041104 (2017).
[3]D. Rhodes, S. Das, Q. R. Zhang, B. Zeng, N. R. Pradhan, N. Kikugawa, E. Manousakis, and L. Balicas, Phys. Rev. B **92**, 125152 (2015).
[4]C. Zhu, F. Wang, Y. Meng, X. Yuan, F. Xiu, H. Luo, Y. Wang, J. Li, X. Lv, L. He, Y. Xu, J. Liu, C. Zhang, Y. Shi, R. Zhang, and S. Zhu, Nat. Commun. **8**, 14111 (2017).
[5]C. Zhu, X. Yuan, F. Xiu, C. Zhang, Y. Xu, R. Zhang, Y. Shi, and F. Wang, Appl. Phys. Lett. **111**, 091101 (2017).
[6]S. Huang, M. Sanderson, J. Tian, Q. Chen, F. Wang, and C. Zhang, J. Phys. D: Appl. Phys. **51**, 015101 (2018).
[7]D. Harris, P. Allen, H. Han, B. Walker, J. Lee, and M. Bawendi, J. Am. Chem. Soc. **133**, 4676 (2011).
[8]Q. Wang, C.-Z. Li, S. Ge, J.-G. Li, W. Lu, J. Lai, X. Liu, J. Ma, D.-P. Yu, Z.-M. Liao, and D. Sun, Nano Lett. **17**, 834 (2017).
[9]M. N. Ali, J. Xiong, S. Flynn, J. Tao, Q. D. Gibson, L. M. Schoop, T. Liang, N. Haldolaarachchige, M. Hirschberger, N. P. Ong, and R. J. Cava, Nature **514**, 205 (2014).
[10]X.-C. Pan, X. Chen, H. Liu, Y. Feng, Z. Wei, Y. Zhou, Z. Chi, L. Pi, F. Yen, F. Song, X. Wan, Z. Yang, B. Wang, G. Wang, and Y. Zhang, Nat. Commun. **6**, 7805 (2015).
[11]Y. M. Dai, J. Bowlan, H. Li, H. Miao, S. F. Wu, W. D. Kong, Y. G. Shi, S. A. Trugman, J.-X. Zhu, H. Ding, A. J. Taylor, D. A. Yarotski, and R. P. Prasankumar, Phys. Rev. B **92**, 161104 (2015).
[12]F. Zheng, C. Cai, S. Ge, X. Zhang, X. Liu, H. Lu, Y. Zhang, J. Qiu, T. Taniguchi, K. Watanabe, S. Jia, J. Qi, J.-H. Chen, D. Sun, and J. Feng, Adv. Mater. **28**, 4845 (2016).
[13]J. Koo, Y. I. Jhon, J. Park, J. Lee, Y. M. Jhon, and J. H. Lee, Adv. Funct. Mater. **26**, 7454 (2016).
[14]M. Gao, M. Zhang, W. Niu, Y. Chen, M. Gu, H. Wang, F. Song, P. Wang, S. Yan, F. Wang, X. Wang, X. Wang, Y. Xu, and R. Zhang, Appl. Phys. Lett. **111**, 031906 (2017).
[15]J. Wang, Z. Jiang, H. Chen, J. Li, J. Yin, J. Wang, T. He, P. Yan, and S. Ruan, Opt. Lett. **42**, 5010 (2017).
[16]M. Pan and H. Yuan, ECS Trans. **75**, 3 (2016).
[17]S. Sim, J. Park, J.-G. Song, C. In, Y.-S. Lee, H. Kim, and H. Choi, Phys. Rev. B **88**, 075434 (2013).
[18]A. Chernikov, C. Ruppert, H. M. Hill, A. F. Rigosi, and T. F. Heinz, Nat. Photonics **9**, 466 (2015).
[19]C. Zhu, Y. Liu, J. Xu, Z. Nie, Y. Li, Y. Xu, R. Zhang, and F. Wang, Sci. Rep. **7**, 11221 (2017).
[20]M. Seo, H. Yamaguchi, A. D. Mohite, S. Boubanga-Tombet, J.-C. Blancon, S. Najmaei, P. M. Ajayan, J. Lou, A. J. Taylor, and R. P. Prasankumar, Sci. Rep. **6**, 21601 (2016).
[21]J. Mangeney, N. Stelmakh, F. Aniel, P. Boucaud, and J.-M. Lourtioz, Appl. Phys. Lett. **80**, 4711 (2002).
[22]C. W. Luo, I. H. Wu, P. C. Cheng, J.-Y. Lin, K. H. Wu, T. M. Uen, J. Y. Juang, T. Kobayashi, D. A. Chareev, O. S. Volkova, and A. N. Vasiliev, Phys. Rev. Lett. **108**, 257006 (2012).
[23]B. Liu, Y. Meng, X. Ruan, F. Wang, W. Liu, F. Song, X. Wang, J. Wu, L. He, R. Zhang, and Y. Xu, Nanoscale **9**, 18546 (2017).
[24]Z. Nie, C. Trovatello, E. Pogna, S. Conte, P. Miranda, E. Kelleher, C. Zhu, E. Turcu, Y. Xu, K. Liu, G. Cerullo, and F. Wang, Appl. Phys. Lett. **112**, 031108 (2018).
[25]Z. Tian, K. Wu, L. Kong, N. Yang, Y. Wang, R. Chen, W. Hu, J. Xu, and Y. Tang, Laser Phys. Lett. **12**, 065104 (2015).
[26]C. Zhao, H. Zhang, X. Qi, Y. Chen, Z. Wang, S. Wen, and D. Tang, Appl. Phys. Lett. **101**, 211106 (2012).